A STUDY ABOUT THE MECHANICAL PROPERTIES OF ALCLAD AA2024 CONNECTIONS PROCESSED BY FRICTION SPOT WELDING[1]

Marco Antônio Durlo Tier[2]
Jorge Fernandes dos Santos[3]
Tonilson de Souza Rosendo[4]
José Antônio Esmerio Mazzaferro[5]
Cíntia Cristiane Petry Mazzaferro[4]
Telmo Roberto Strohaecker[4]
Luciano Andrei Bergmann[3]
Cesar Afonso Weis Olea[6]
Antônio da Silva[7]

Abstract
Friction Spot Welding – FSpW, also known as Refill Friction Spot Welding is a new solid-state spot process developed by GKSS, exhibiting as one of the main advantages, no key-hole on the surface of the material after the completion of the process. In the present work FSpW has been performed in 2 mm-thick Alclad AA2024-T3 varying tool rotational speeds, sleeve plunge depths and plunge rates. Mechanical properties of the connections have been investigated in terms of hardness and shear testing. The fracture mechanisms were observed by SEM and the microstructural features by OM. The results have demonstrated that the optimum tool rotational speed is dependent on the other welding parameters as plunge rate and plunge depth. Plunge depths of around 25% (0.5 mm) in the bottom plate thickness have proved to be adequate to reach a good mechanical performance of the connections. It was observed that the main feature affecting the mechanical properties of the joint is the Alclad distribution inside the weld. Furthermore, lower plunge rates have resulted in more homogeneous distribution of the Alclad and thus, in better mechanical performance of the connections.
Key words: Friction spot welding; FSpW; AA 2024; Alclad; SEM.

ESTUDO DAS PROPRIEDADES MECÂNICAS DE JUNTAS DE ALUMÍNIO ALCLAD AA2024 PROCESSADAS PELO PROCESSO DE SOLDA PONTUAL POR FRICÇÃO – FSpW

Resumo
A técnica de solda pontual por fricção (Friction Spot Welding – FSpW), também conhecida como Refill Friction Spot Welding é um novo processo de solda pontual no estado sólido desenvolvido pelo GKSS, exibindo como uma das principais vantagens, a inexistência de cavidade na superfície do material, após a finalização do processo. Neste trabalho, FSpW foi realizado em chapas de 2mm de espessura da liga Alclad AA2024-T3 variando-se a velocidade de rotação da ferramenta, profundidade de penetração e taxa de penetração do sleeve (ombro). As propriedades mecânicas das juntas foram investigadas em termos de dureza e resistência ao cisalhamento. Os mecanismos de fratura foram analisados utilizando-se MEV enquanto a microestrutura foi investigada por MO. Os resultados obtidos demonstraram que a velocidade de rotação ótima da ferramenta é dependente dos outros parâmetros de processo como profundidade e taxa de penetração. Profundidades de penetração em torno de 25% (0.5 mm) na chapa inferior provaram serem satisfatórias para se obter uma boa performance mecânica das juntas. Observou-se que a principal fator a afetar as propriedades mecânicas das juntas é a distribuição de Alclad no interior da solda. Além disso, menores taxas de penetração resultaram em uma distribuição mais homogênea do Alclad e desta forma, em melhor performance mecânica das juntas soldadas.
Palavras-chave: Solda pontual por fricção – FSpW; AA 2024; Alclad; MEV.

[1] *Technical contribution to 64th ABM Annual Congress, July, 13th to 17th, 2009, Belo Horizonte, MG, Brazil.*
[2] *Departamento de Engenharias e Ciência da Computação, DECC - URI – Santo Ângelo, RS, Brazil, Marco.Tier@urisan.tche.br.*
[3] *GKSS Research Centre, Institute of Materials Research, Materials Mechanics, Solid State Joining Processes, Geesthacht, Germany.*
[4] *DEMET/PPGEM - UFRGS, Porto Alegre, RS, Brazil.*
[5] *DEMEC/PROMEC - UFRGS, Porto Alegre, RS, Brazil.*
[6] *Vallourec & Mannesmann Tubes, Belo Horizonte, MG, Brazil*
[7] *LORTEK – Centro de Investigation em Tecnologias de Union, Ordizia, Spain.*

1 INTRODUCTION

In the past few years an increasing use of lightweight materials has been observed in the automotive and aerospace industries, aiming both fuel saving and safety. As a result, many components produced from lightweight alloys (specially aluminum and magnesium alloys) by stamping, casting, extrusion and forging, have to be joined as part of manufacturing processes. Currently most spot-like joints for automotive and aeronautic structural components are made by mechanical fastening (clinching, riveting, self-piercing riveting), resistance spot (RSW) and laser spot welding as well as by other processes, such as weld-bonding.[1-4] Mechanical fastening suffers from a weight penalty, difficult of automation, need of sealants and is subject to corrosion problems.

For resistance and laser spot welding there are significant problems especially in the high strength aluminum alloys related to the oxide/hydroxide layer and dissolved hydrogen. So far, RSW in aluminum has the tendency to produce low quality welds. Furthermore, there are high operating costs, since the higher electrical and thermal conductivities of aluminum lead to higher energy consumption, demanding powerful electrical systems and associated infrastructure.[5,6] Another disadvantage is the reduction in the electrode tip life, which results in a decrease of the weld quality and hence, in poor mechanical behavior.[7]

In the recent years, FSpW and other solid-state spot welding techniques such as friction stir spot welding (FSSW) have received considerable attention from the automotive and aircraft industries since such processes offer an alternative to overcome the disadvantages presented by conventional welding.[3-13] It can also be an alternative for long friction stir welds (FSW) in aluminium thin sheets. Furthermore, where riveting could be replaced by spot welding techniques a great reduction of weight can be achieved. FSpW can also be used for the repair of surface defects and for filling the keyhole resulting from friction stir welding.[14]

2 EXPERIMENTAL PROCEDURE

Formatados: Marcadores e numeração

2.1 Material

The Alclad AA2024-T3 2mm sheets have been used to produce the welds in overlap configuration. Table 1 presents the chemical composition of the material. The pure aluminum layer, on both top and bottom surfaces of the sheets, was approximately 100 µm thick.

Table 1. Chemical composition of the Alclad AA 2024-T3

Grade	Si	Fe	Cu	Mn	Mg	Zn	Ti	Al
2024	0.19	0.23	3.94	0.55	1.24	0.22	0.02	bal.

2.2 Welds

FSpW connections have been processed by RIFTEC GmbH at GKSS Research Centre (Geesthacht, Germany) using a FSpW prototype unit capable of applying forces up to 7.8 kN (vertical axis) and with maximum rotational speed of 3000 rpm.

The FSpW process[15-22] is performed by plunging a rotating tool into the workpiece, which produces frictional heat on the upper sheet surface. The tool consists of a three-piece system named clamping ring, sleeve and pin, as illustrated

in Figure 1. Each one of these pieces has an independent actuation system and therefore, they can be moved up and down independently. The pin and sleeve are moved in opposite vertical direction to each other while the stationary clamping ring holds the work piece in the proper position during processing.

The effect of three process parameters on the weld joint has been investigated: sleeve plunge depth, sleeve rotational speed and plunge rate (welding time), see Table **2**. The total welding time comprises the plunge and retract times. No dwell time has been used. Both pin and sleeve have been retracted as soon as the required plunge depth has been achieved.

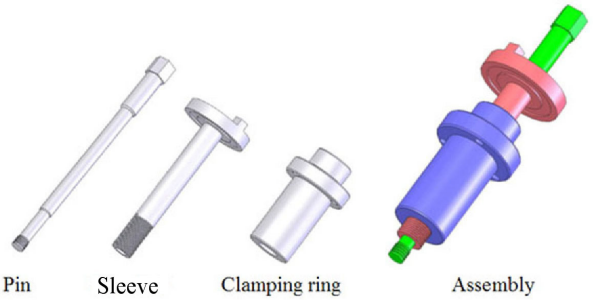

Figure 1. Schematic illustration of the three-piece tool system in FSpW: clamping ring, sleeve and pin.

Table 2. Parameters used to produce the connections

Sleeve Plunge Depth	2.2, 2.5, 2.8 mm (0.2, 0.5, 0.8 mm in bottom sheet)		
Sleeve Plunge Rate	From 0.82 to 1.87 mm/s		
Sleeve Rotational Speed	1900 rpm	2400 rpm	2900 rpm

There are two variants of the FSpW process: “pin plunge”, when the pin is plunged into the material while the sleeve is retracted, and “sleeve plunge” when the sleeve plunges into the material while the pin is retracted. In the present work, it was used the “sleeve plunge variant” which compared to “pin plunge variant” presents the advantage of a larger welded area as a consequence of a larger cross section of the sleeve. On the other hand, it demands a higher plunging force.

The first stage of the process (Figure 2 (a)), consists of rotating and moving the sleeve and the pin towards the plate with an angular velocity “ϖ”, while the clamp keeps the sheets held tightly. In the second stage (Figure 2 (b)), the sleeve and pin move with linear vertical velocity “Vp” (pin velocity) and “Vs” (sleeve velocity). The sleeve starts plunging into the plates until a preset plunge depth. The pin moves up creating a cavity to accommodate the plasticized material displaced by the sleeve.

The relationship between “Vp” and “Vs” is adjusted in order to keep constant the volumetric displacement of the pin and the shoulder. Depending on the tool design, part of the displaced material may escape through a gap between the clamp and the sleeve. In this case some amount of flash may be formed.

The third stage (Figure 2 (c)), consists of the sleeve and the pin retracting back, towards the surface of the plate, pushing back the material initially displaced, to the surface level. In the fourth stage (Figure 2 (d), the process is completed leaving completely “refilled” hole with minimal or no surface indentation, since material loss is almost imperceptible.

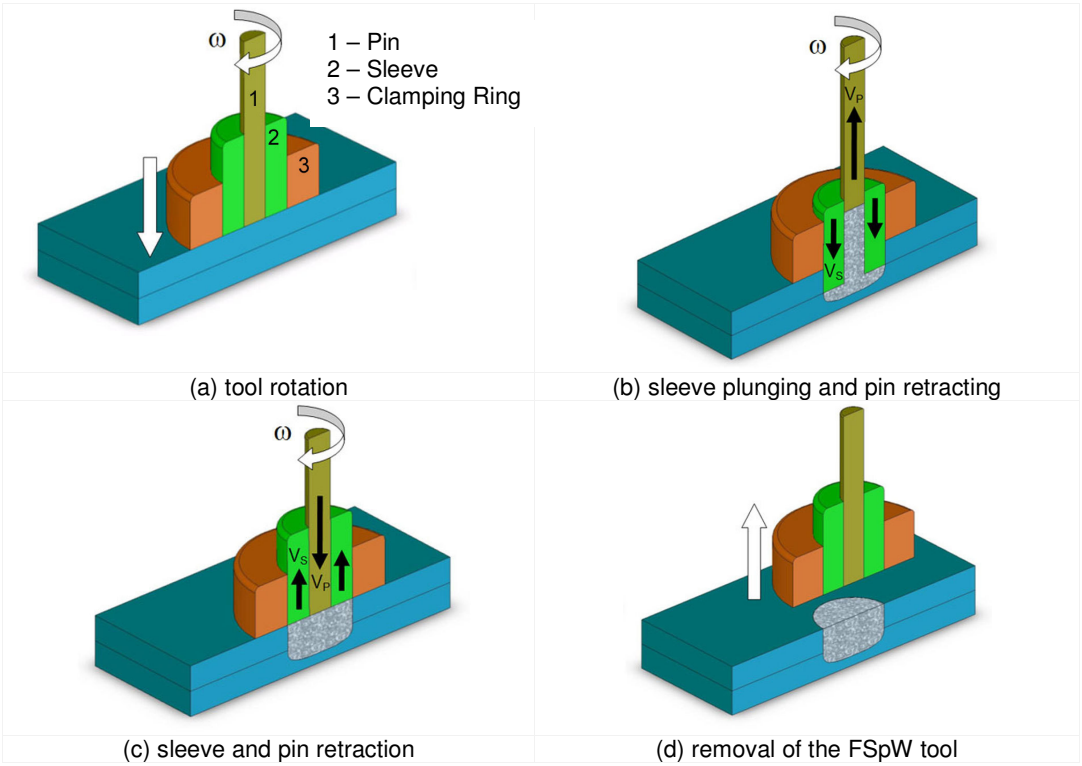

Figure 2. Schematic illustration of the four main stages of FSpW process (sleeve plunge variant): (a) tool rotating and clamping, (b) sleeve plunging and pin retracting, (c) pin plunging and sleeve retracting and (d) removal of the FSpW tool.

2.3 Analysis

Light optical microscopy (OM) has been used to investigate the microstructural features within the FSpW connections. Samples have been prepared according to standard metallographic procedures and etched using Kroll solution (96 ml H_2O, 6 ml HNO_3 and 2 ml HF). Shear tests have been carried out using 230 x 60 mm specimens (46 mm overlap) according to DIN EN ISO 14273:2002 standard[(32)] (Figure 1). Shims of the same material and thickness as the test specimens have been used when clamping the samples to induce pure shear and to avoid the initial realignment during testing. The equipment utilized was a screw-driven testing Schenck Trebel RM100 machine powered by a Zwick controller (100 kN load capacity) with displacement rates between 1 and 2 mm/min. The fracture mechanisms have been analyzed by scanning electron microscopy (SEM).

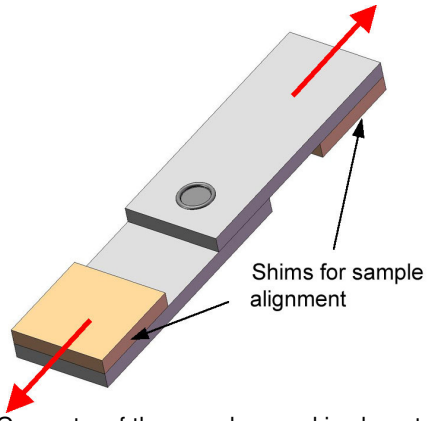

Figure 1. Geometry of the samples used in shear test.

3 RESULTS AND DISCUSSION

3.1 Shear Test

Table 3 presents the results of the shear tests. The first two columns indicate the nomenclature for each set of weld parameters (weld condition) and the tool rotational speed, respectively. The third and fourth columns show the sleeve plunge depth and the plunge rate. The fifth column presents the total time of the process, which is dependent of the plunge rate. Half of the time was spent during material penetration (plunge stage) and half during the retraction of the tool. Finally, the last two columns present the average shear strength and standard deviation (SD) for the actual weld condition.

Three shear tests replicates were performed for each weld condition indicated as “A”, “B” and “C”. During the shear test occasionally there would be a problem with the machine apparatus and then the result of that sample was discarded. The green color is used to emphasize the best mechanical performance while the red color is used to emphasize the worst connections. It is worth noting that for most of the weld conditions the standard deviation was very high. As examples, we can emphasize weld condition S12 (SD 1.93), S2 (SD 1.74), S9 (SD 1.69) and S10 (SD 1.68).

The best mechanical performance is found for weld condition S15 (10.68 KN) processed at 1900 rpm, plunge depth: 2.5 mm (0.5 mm = 25% penetration in bottom sheet), plunge rate: 1.04 mm/s (4.8 s). The worst four connections in terms of shear load (S2, S3, S4, S6) have been processed with plunge depth of 2.2 mm (0.2mm =

10% in bottom sheet), suggesting that the penetration is not enough to produce a good bonding between the two sheets.

Table 3. Results from shear test for Alclad AA2024-T3 FSpW

Alclad AA 2024 – T3									
Weld Cond	RPM	PDepth	PRate	Time	Max Shear Load (KN)				
	Plunge	(mm)	mm/s	Total (s)	A	B	C	Aver	S. D.
S1	2900	2.20	1.57	2.80	10.03	-----	9.85	9,94	0.13
S2	2400	2.20	1.57	2.80	6.08	8.33	4.90	6.44	1.74
S3	1900	2.20	1.57	2.80	7.15	5.59	6.77	6.50	0.81
S4	2900	2.20	1.16	3.79	7.80	6.43	6.63	6.95	0.74
S5	2400	2.20	1.16	3.79	8.18	9.35	8.53	8.69	0.60
S6	1900	2.20	1.16	3.79	5.83	6.81	7.37	6.67	0.78
S7	2900	2.20	0.92	4.78	8.00	8.40	6.40	7.60	1.06
S8	2400	2.20	0.92	4.78	9.26	9.62	9.61	9.50	0.21
S9	1900	2.20	0.92	4.78	9.56	6.23	8.35	8.05	1.69
S10	2900	2.50	1.32	3.79	7.13	10.14	7.35	8.21	1.68
S11	2400	2.50	1.32	3.79	8.73	8.73	9.03	8.83	0.17
S12	1900	2.50	1.32	3.79	7.69	11.19	8.03	8.97	1.93
S13	2900	2.50	1.04	4.81	-------	7.02	7.89	7,45	0.61
S14	2400	2.50	1.04	4.81	8.45	7.71	8.89	8.35	0.60
S15	1900	2.50	1.04	4.81	10.46	10.16	11.42	10.68	0.66
S16	2900	2.50	0.86	5.81	8.45	8.26	9.63	8.78	0.74
S17	2400	2.50	0.86	5.81	9.17	8.62	7.72	8.50	0.73
S18	1900	2.50	0.86	5.81	7.93	10.66	10.19	9.59	1.46
S19	2900	2.80	1.16	4.78	8.07	8.10	9.65	8.61	0.90
S20	2400	2.80	1.16	4.78	9.85	9.61	7.97	9.14	1.02
S21	1900	2.80	1.16	4.78	8.27	9.19	8.11	8.52	0.58
S22	2900	2.80	0.96	5.81	8.68	9.61	8.28	8.86	0.68
S23	2400	2.80	0.96	5.81	10.52	8.62	10.24	9.80	1.03
S24	1900	2.80	0.96	5.81	9.69	9.60	8.08	9.12	0.90
S25	2900	2.80	0.82	6.83	9.23	7.58	9.60	8.80	1.07
S26	2400	2.80	0.82	6.83	7.16	9.66	8.26	8.36	1.25
S27	1900	2.80	0.82	6.83	7.46	8.36	7.32	7.71	0.56

In order, to a better visualization of the mechanical performance of the connections, Figure 2 presents the results in a graphic chart. The value used for shear load represents the average of the 3 samples. It is possible to observe that plunge rate plays an important role in the shear performance of the Alclad AA2024-T3 FSpW. Lower plunge rate (around 0.9 to 1.05 mm/s) usually resulted in higher shear loads, while higher plunge rate usually resulted in lower shear load see Figure 2 (b) and (c). However, weld condition “S1” with plunge rate of 1.57 mm/s (2900 rpm) and good performance represents an exception for this statement, (Figure 2 (a). These results are in disagreement with FSpW of AA5042 [21] where it was observed a weak influence of the plunge rate in the mechanical behavior of the connections.

When it is analyzed the effect of tool rotational speed it is possible to observe that for plunge depth of 2.2mm (Figure 2a) the highest shear load is associated with rotational speed of 2900 rpm. For plunge depth of 2.5mm (Figure 2b) the highest shear load is associated with rotational speed of 1900 rpm while for plunge depth of 2.8 mm the highest shear load is associated with speed of 2400 rpm. These results suggest that the optimum rotational speed is dependent of the other process variables as plunge rate and plunge depth.

Figure 3 (a) shows that when plunge depth is increased from 2.2 mm to 2.8 mm significant benefit is reached. However, no benefit is observed when plunge depth is increased from 2.5 mm to 2.8 mm (Figure 3 (b). The best connections in terms of shear load were processed with plunge depth varying between 2.5 mm to 2.8 mm (0.5 mm to 0.8 mm in bottom sheet). These results are in good agreement with common practice when making FSW lap welds that is to penetrate the bottom sheet around 30% of its thickness.[33]

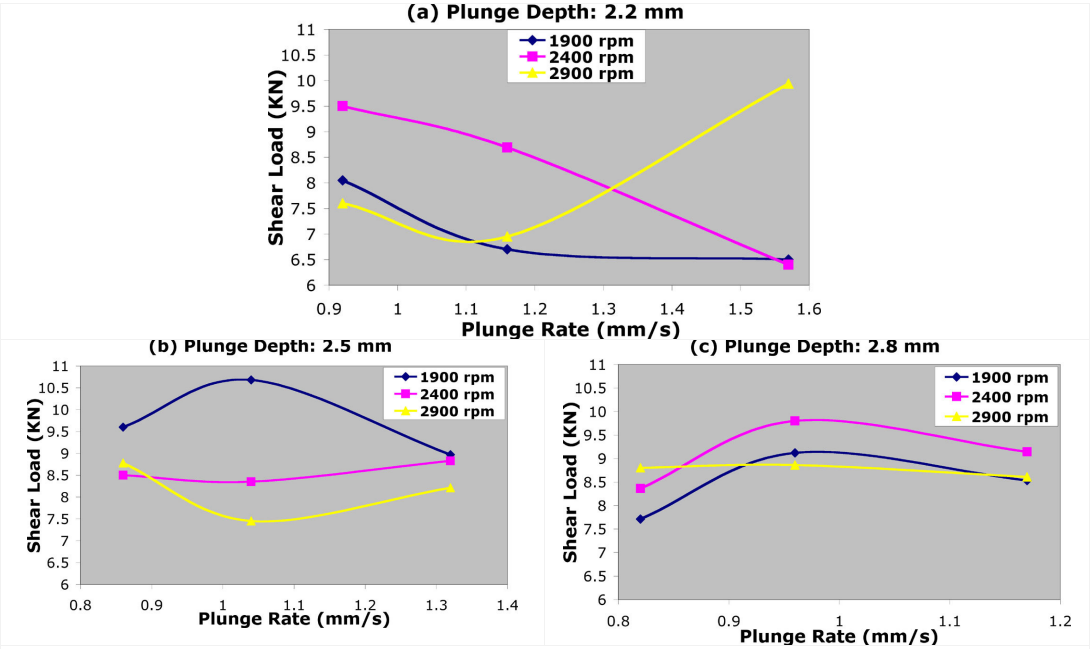

Figure 2. Mechanical performance of the FSpW connections in shear test.

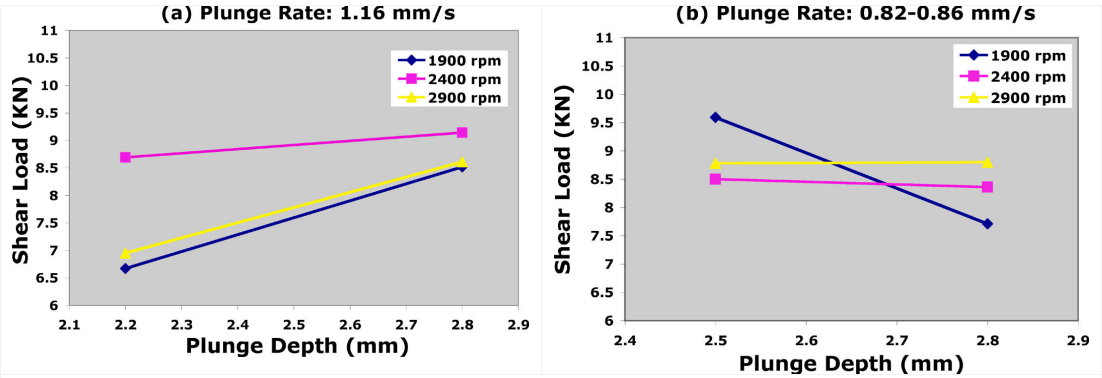

Figure 3. Effect of plunge depth in shear load.

3.2 Microstructural Characterization

Figure 4 presents the cross section view of the connection S1 while Figure 5a shows a close-up view of the right lower corner the interface SZ/TMAZ. It can be observed that the Alclad layer is partially broken up and tends to move towards the stir zone (SZ). Figure 5b apparently shows that in some regions of the SZ there is a poor mixing of Alclad with the plasticized material resulting in a formation of Alclad islands. Therefore, one may expect a non-uniform strength distribution inside the SZ region.

Figure 6 presents additional macrographs for some “high strength” and “low strength” connections. Although Alclad particles are observed in the SZ for all joints, their distributions do not follow the same pattern.

Figure 4. Cross section of the connection “S1” processed at: 2900 rpm, plunge depth 2.2 mm (0.2 mm), plunge rate 1.57 mm/s, time 2.8 s. Etching: Kroll solution.

(a) Interface of the SZ with the TMAZ

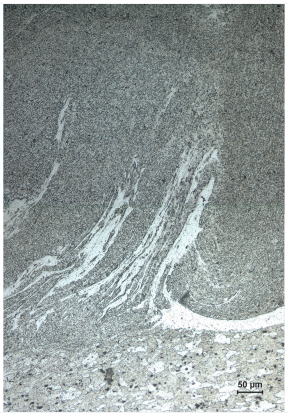

(b) SZ showing the presence of Alclad

Figure 5. Higher magnification of the cross section of connection “S1“ presented in Figure 4. (a) Interface between stir zone (SZ) and thermo-mechanically effected zone (TMAZ) and (b) low right corner of SZ.

High Strength Connections

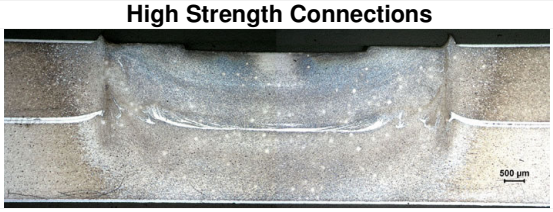

(a) Connection “S23” processed at: 2400 rpm, plunge depth 2.8 mm, plunge rate 0.96 mm/s, time 5.8 s

Low strength Connections

(c) Connection “S2” processed at 2400 rpm, plunge depth 2.2 s, plunge rate 1.57 s, time 2.8 s.

(b) Connection “S15” processed at: 1900 rpm, plunge depth 2.5 mm, plunge rate 1.04 mm/s, time 4.8s.

(d) Connection “S3” processed at 1900 rpm, plunge depth 2.2 s, plunge rate 1.57 mm/s, time 2.8 s.

Figure 6. Cross section of “high strength“ and “low strength“ connections observed in optical microscopy. Etching: Kroll.

Erro! Fonte de referência não encontrada. presents the hardness profile through the stir zone for the weld condition “S8”. The hardness line-profiles were performed: the first line at approximately 0.5 mm, the second at 1.25 mm and the third at 1.75 mm from the top surface. In order to avoid superposition, it was added a Δ of 20HV to the top line and subtracted a Δ of 30 HV from the bottom line. It can be observed a minor increase in hardness inside of the stir zone and a slight softening outside the welded area in a region where it is believed to be located the heated affected zone (HAZ).

It is worth noting that for the bottom line there are significant drops of hardness in some points. This phenomenon is associated with the presence of Alclad particles inside the stir zone.The presence of Alclad islands inside the stir zone could be a reasonable explanation for the significant scattering in strength values between connections processed with the same parameters. This feature will be further analyzed in next section: fracture mechanisms.

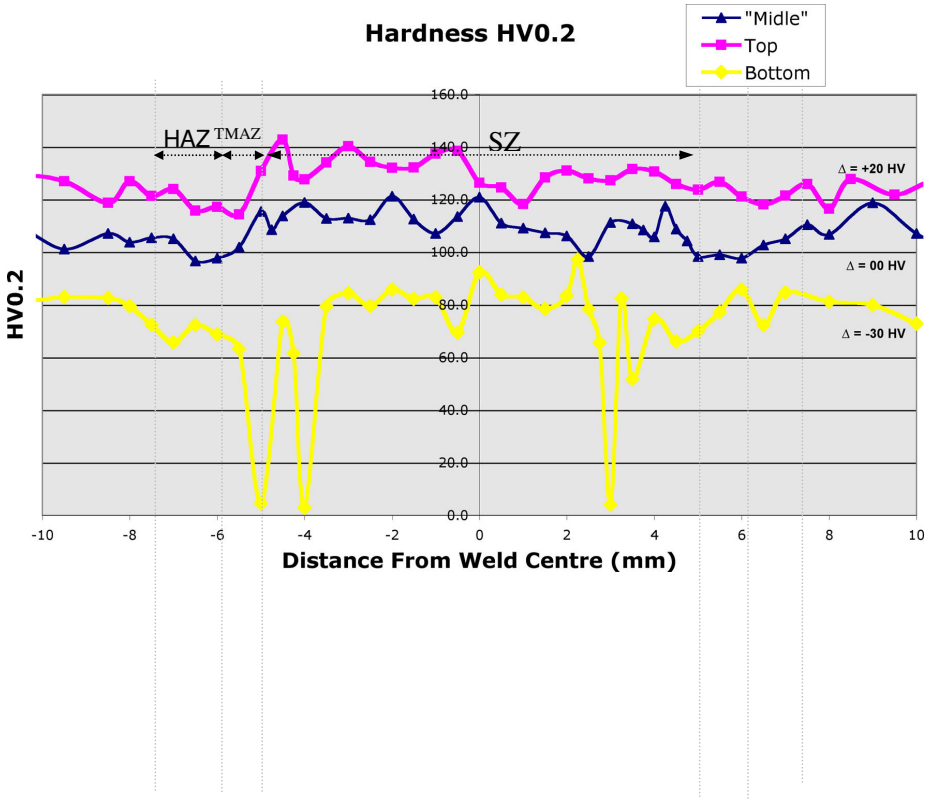

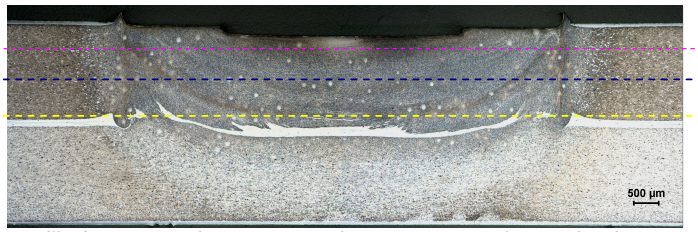

Figure 9. Hardness profile for connection processed at 2400 rpm, plunge depth 2.2 mm, time 4.8 s, plunge rate 0.92 mm/s.

3.3 Fracture Mechanisms

Figure 10 shows the fracture surface in the SZ for specimen 9B. This specimen had through weld fracture mode and low shear strength (Table 3). There are localized areas presenting coarsened cavities (dimples) indicating the presence of secondary phases. Therefore, it is expected the occurrence of islands of Alclad in SZ. However EDX analysis was not successful in differentiate the chemical composition of Alclad particles and AA2024-T3 material, due to limited hardware resolution.

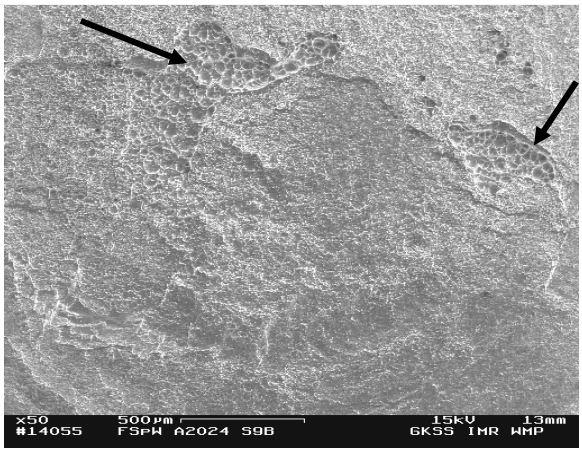

50X

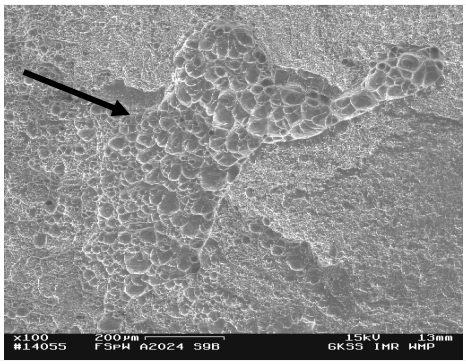

100X

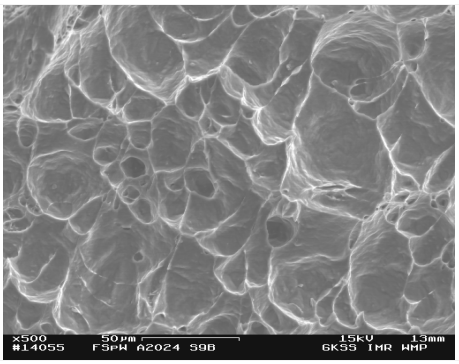

500X

Figure 7. Center of the SZ after the shear test for connection „S9B“ (low strength) processed at: 1900 rpm, plunge depth 2.2 mm, time:3.8 s, plunge rate 0.92mm/s. There is localized ductile behavior evidenced by coarsened cavities suggesting a secondary phase in the SZ.

Furthermore, Figure 11 also shows the existence of a ring of large dimples at the interface SZ/TMAZ for specimen 9B (low strength). However, sample “9A” (high strength) processed with the same set of parameters of specimen “9B” presented

shear load much higher and the localized coarsened cavities are not observed (Figure 12). Although, the fracture mode is similar for both specimens (through weld) the fracture aspect is totally different.

The authors believe that the process parameters have an important influence on the Alclad distribution. However, according to shear tests and SEM analyses, it seems that even using the same set of parameters, differences in the homogeneity of Alclad distribution can be produced. For some specimens it seems that Alclad is more concentrated in some regions of the SZ with a reduction in strength, while for others specimens, the Alclad appears to be more evenly stirred in the SZ with a consequent improvement in the strength. Therefore, it is important to select a set of process parameters that results in a more homogeneous distribution of the Alclad inside the SZ. It seems that a plunge depth in the range of 25% to 30% of penetration in the bottom sheet and lower plunge rate (0.9 mm/s to 1.05 mm/s) have fulfilled this requirement. In this case there is a longer time for processing and it is expected a more homogeneous distribution of the Alclad layer in the SZ.

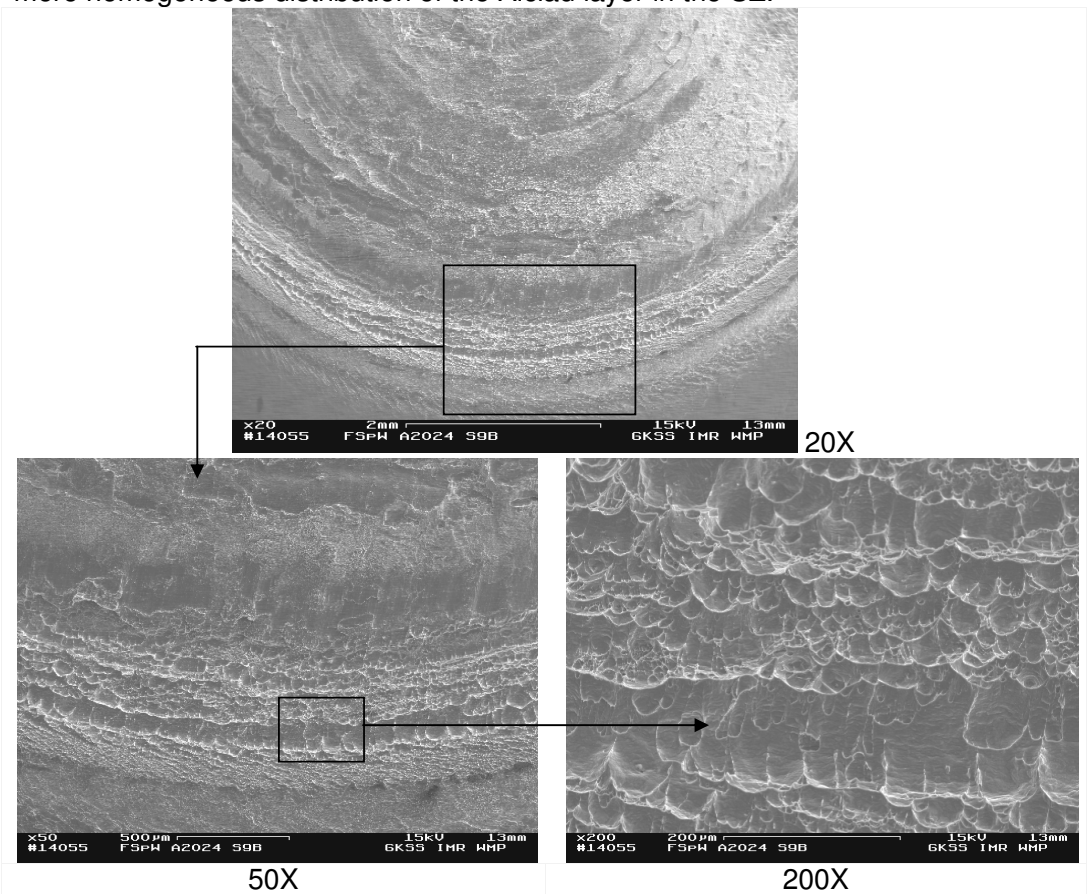

Figure 8. Border of the stir zone at the interface SZ/TMAZ connection „S9B“ (low strength) processed at: 1900 rpm, plunger depth 2.2 mm, plunge rate 0.92mm/s, time 3.8 s. There is ring of dimples suggesting the presence of islands of Alclad material.

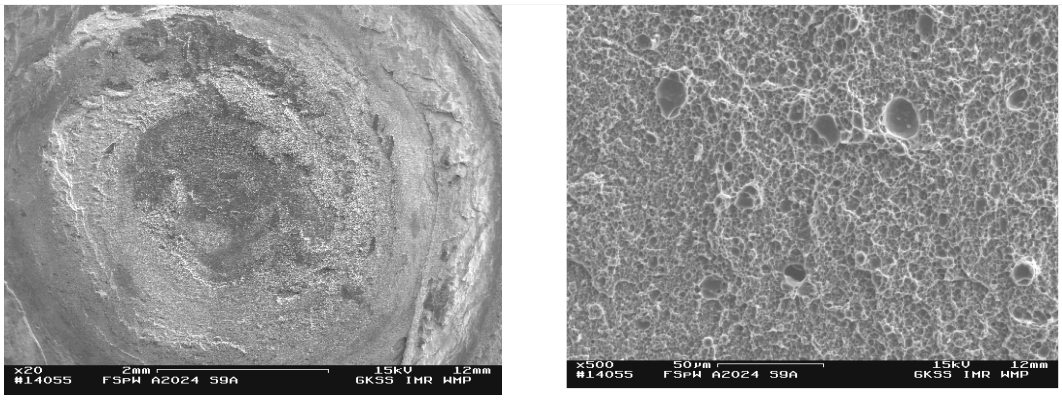

(a) 20 X (b) 500 X

Figure 9. Center of the SZ after the shear test for connection "S9A" (high strength) processed at: 1900 rpm, plunge depth 2.2 mm, time: 3.8 s, plunge rate 0.92mm/s. No coarsened cavities are observed.

The present results are in good agreement with work reported by Tweedy et al.[30] They proposed that deeper plunge depth incentives to break up the clad material. Furthermore, there is also a good agreement with the results from Ali et al.[23] and from Booth and Sinclair[24] about fatigue of friction stir welded 2024-T351. They have observed that failure in the stir zone (SZ) is associated with material discontinuities resulting in much lower mechanical performance of the weld, when compared to failure from TMAZ or HAZ.

4 CONCLUSION

Formatados: Marcadores e numeração

The choice of the optimum tool rotational speed appears to be dependent on the other FSpW process parameters as plunge rate and plunge depth.
The plunge depth of 0.2 mm (10%) in the lower sheet was inadequate in most of the connections while plunge depths around 0.5 (25 % of sheet thickness) demonstrate to be satisfactory in terms of shear performance of the connections.
As general tendency, lower plunge rates (0.90 mm/s to 1.05 mm/s) resulted in better shear performance of the connections.
The Alclad layer plays an important role in the shear performance of AA 2024 FSpW. The better mechanical performance of the connections was associated with process parameters that resulted in a more homogeneous distribution of Alclad in the SZ.

Acknowledgments

Capes and CNPq Brazilian Government Founding.
RIFTEC GmbH by producing the FSpW connections.
Mr U. Lorenz for supporting in SEM facilities and Mrs P. Fisher for supporting in metallographic preparation.
Dr G. Pinheiro and Dr S. Amancio for important suggestions for the work.

REFERENCES

1 Han L, Young K.W, Chrysantou A, O'Sullivan J.M, The Effect of Pre-Straining on the Mechanical Behaviour of Self-Piercing Riveted Aluminium Alloy Sheets, Materials and Design 27 (2006), 1108-1113.

2 Kahraman N, The Influence of Welding Parameters on the Joint Strength of Resistance Spot-Welded Titanium Sheets. Materials and Design 28 (2007), 420-427.
3 Su P, Gerlich A, North T.H, Bendszak G.J. Energy Utilisation and Generation During Friction Stir Spot Welding. Science and Technology of Welding and Joining 11 (2006), 163-169.
4 North T.H, Bendszak G.J, Gerlich A, Su P, Cingara G, Transient Local Melting in Al 7075-T6 Friction Stir Spot Welds. Materials Science Forum 539-543 (2007), 3826-3831.
5 Mazda media release. Mazda Develops World´s First Steel and Aluminum Joining Technology Using Friction heat. June 2, 2005. http://www.mazda.com/publicity/release/2005/200506/050602.html
6 Gerlich A, Avramovich-Cingara G, North T.H, Stir Zone Microstructure and Strain Rate during Al 7075-T6 Friction Stir Spot Welding, Metallurgical and Materials Transactions A 37A (2006), 2773-2786.
7 Zhou Y, Fukomoto S, Peng J, Ji C.T, Brown L, Experimental Simulation of Surface Pitting of Degraded Electrodes in Resistance Spot Welding of Aluminium Alloys, Materials Science and Technology 20 (2004), 1226-1232.

8 Hinrichs J.F, Smith C.B, Orsini B.F, DeGeorge R.J, Smale B.J, Ruehl P.C, Friction Stir Welding for the 21st Century Automotive Industry, Proceedings of the 5th International Symposium on Friction Stir Welding, September 14–16, 2005, Metz, France.
9 Ross H, Friction Welding of Aluminium Cuts Energy Costs by 99%, Welding Journal 83 (2004), 40.
10 Mazda Media Release. Mazda Develops World's First Aluminum Joining Technology Using Friction Heat, February 27, 2003. http://www.mazda.com/publicity/release/2003/200302/0227e.html
11 Gerlich A, Avramovich-Cingara G, North T.H, The Influence of Processing Parameters on Microstructure of Al 5754 Friction Stir Spot Welds, Materials Science Forum 519-521 (2006), 1107-1112.
12 Kiffin W.J, Threadgill P.L, Lalvani H, Wynne B.P, Progress in FSSW of DP800 High Strength Automotive Steel, Proceedings of the 6th International Symposium on Friction Stir Welding, October 10–13, 2006, Montreal, Canada.
13 Su P, Gerlich A, North T.H, Bendszak G.J, Material Flow during Friction Stir Spot Welding, Science and Technology of Welding and Joining 11 (2006), 61-71.
14 Arbegast W.J, Allen C.D, Langerman M, Marquis F, Henderson E, Svedin C, Moore C, Trujillo A, Podraza D, Freeman J, Koch N, An Investigation of Friction Spot Welding of Thin Aluminium Sheets, Proceedings of the 15th AEROMAT - Advanced Aerospace Materials and Processes Conference, June 7-10 2004, Seattle, USA.
15 Schilling C, Dos Santos J, Method and device for joining at least two adjoining work pieces by friction welding, Patent No. US 6,722,556 B2, April 20, 2004.
16 Da Silva A, Tier M. D, Rosendo T, Mazzaferro C, Mazzaferro J, Ramos F.D, Beyer M, Bergmann L, Isakovic J, Strohaecker T.R, Dos Santos J.F, Microstructure and Properties of Friction Spot Welds in a 2-mm Thick Alclad AA 2024-T3, FABTECH & AWS Welding Show, Chicago - IL, USA, November 11-14, 2007.
17 Silva A, Tier M. D, Rosendo T, Ramos F.D, Mazzaferro C, Mazzaferro J, Bergmann L, Strohaecker T.R, Dos Santos J.F, Friction Spot and Friction Stir Spot Welding Processes – A Literature Review, Bulletin of National R&D Institute for Welding and Material Testing, ISSN 1453-0392, 3/2007, 36-44.
18 Rosendo T, Da Silva A.M, Tier M.D, Dornelles F, Mazzaferro J.A.E, Mazzaferro C.P, Dos Santos J.F, Strohaecker T.R, Preliminary Investigation on Friction Spot Welding of Alclad 2024-T4 Aluminum Alloy. XXXIII CONSOLDA, Caxias do Sul – RS, Brazil, 27 – 30 August 2007.
19 Silva A.M, Tier M.D, Rosendo T, Ramos F.D, Beyer M, Strohaecker T.R, Dos Santos J.F, Preliminary investigations on Microstructural features and Mechanical Performance of Friction Spot Welding of Aluminium alloys, IIW International Seminar on Friction based

Spot Welding Processes, 29-30 March (2007), GKSS Forschungszentrum, Geesthacht, Deutschland.
20 Arbegast W.J, Refill Friction Stir Spot Welding of Aluminum Alloys, IIW International Seminar on Friction Based Spot Welding Processes, 29-30 March (2007), GKSS Forschungszentrum, Geesthacht, Deutschland.
21 Tier M.D, Rosendo T, Olea C.W, Mazzaferro C.P, Ramos F.D, Bayer M, Dos Santos J.F, Da Silva A.M, Mazzaferro J. and Strohaecker T.R, The Influence of Weld Microstructure on Mechanical Properties of Refill Friction Spot Welding of 5042 Aluminium Alloy, Proceedings of the 7th International Symposium on Friction Stir Welding, 20-22nd May (2008), Awaji Island, Japan.
22 J. A. E. Mazzaferro, T. Rosendo, C. C. P. Mazzaferro, F. D. Ramos, M. D. Tier, J. F. dos Santos, T. R. Strohaecker. Preliminary investigation on the mechanical behaviour of aluminium friction spot welds, 7th International symposium on friction stir welding, Awaji Island, Japan, 20-22 May, 2008.
23 Ali A, Brown M.W, Rodopoulos C.A. and Gardiner S, Characterization of 2024-T351 Friction Stir Welding Joints, Journal of Failure Analysis and Prevention, Vol 6 (4) August (2006), 83-96.
24 Booth D. and Sinclair I, Fatigue of friction stir welded 2024-T351 Aluminium Alloy, Materials Science Forum, Vols 396-402 (2002), Aluminium Alloys (2002), 1671-1676.
25 Gerlich A, Su P, Yamamoto M and North T. H, Effect of Welding Parameters on The Strain Rate and Microstructure of Friction Stir Spot Welded 2024 Aluminum Alloy, Journal of Materials Science Vol 42 No 14, July 2007, 5589-5601.
26 Chang W.S, Cho H.J, Kim H.J, Chun C.K, Evaluation of Friction Spot Joining Weldability of Al Alloy for Automotive, Material Science Forum Vols 539-543 (2007), 411-416.
27 Freeney T.A, Sharma S.R, Mishra R.S, Effect of Welding Parameters on Properties of 5052 Al Friction Stir Spot Welds, 2006 SAE congress, Detroit, SAE Technical paper 2006-01-0969. Book number SP 2034.
28 Mishra R.S, Freeney T.A, Webb S, Chen Y.L, Garden X.Q, Herlinh D.R. and Grant G.J, Friction Stir Spot Welding of 6016 Aluminum Alloy, Friction Stir Welding and Processing IV, TMS 2007, 341-347.
29 Okamoto K, Hunt F, Development of Friction Stir Welding Technique and Machine for Aluminum Sheet Metal Assembly – Friction Stir Welding of Aluminum for Automotive Applications (2), 2005-01-1254, 2005 SAE Congress, Detroit, SAE Technical paper SP-1959, p 121-125.
30 Tweedy B.T, Widener C.A, Burford D.A, The Effect of Surface Treatments on the Faying Surface of Friction Stir Spot Welds, Friction Stir Welding and Processing IV, TMS (2007), 333-340.
31 Patnaik A. K, Koch K.J, Arbegast W.J, Allen C.D, Static Properties of "Refill" Friction Spot Welded Skin Stiffened Compression Panels, 2006-01-0967, SP 2034.
32 DIN EN ISO 14273, Specimen Dimensions and Procedure for Shear Testing Resistance Spot, Seam and Embossed Projection Welds, 2000.
33 Addison A.C, Robelou A.J, Friction Stir Spot Welding: Principal Parameters and Their Effects, Proceedings of the 5th International Symposium on Friction Stir Welding, 14-16 September 2004, Metz, France.
34 Allen C, Arbergast W. J, Evaluation of Friction Spot Welds in Aluminum Alloys, 2005 SAE Congress, Detroit, SAE Tech. paper SP-1959, 2005-01-1252, p 107-113.